Engineering and Technology Journal
Journal homepage: https://etj.uotechnology.edu.iq

Applying Nanocomposite Coatings to Improve Orthopedic Alloys by Using Multiple Flame Spray

Shahad A. Jabbar[a]*, Niveen J. Abdulkader[a], Payman S. Ahmed[b]

[a]Materials Engineering Dept., University of Technology-Iraq, Alsina'a street, 10066 Baghdad, Iraq.
[b]Manufacturing & Industrial Engineering Dept., Faculty of Engineering, Koya University, Koya KOY45, Kurdistan Region- F.R.Iraq.
*Corresponding author Email: mae.20.73@grad.uotechnology.edu.iq

HIGHLIGHTS

- CoCrNb and CoCrSi alloys were sprayed with multiple torch flames to apply of Nano-coatings (A: 75% HAP+ 25% SiC, and B: 75% Zeolite+ 25% ZrO_2)
- The zeolite+ZrO_2 (type B) and HAP+SiC (type A) coating layers act as barriers to the release of Co and Cr ions from CoCr alloys.
- CoCrSi coated type B are the best to be implanted where the cytotoxicity is 0% in the human body

ARTICLE INFO

Handling editor: Akram R. Jabur

Keywords:
CoCrNb
CoCrSi
Coating
HAP+SiC
Zeolite+ZrO_2

ABSTRACT

Due to their excellent mechanical and biocompatibility characteristics, CoCr-based alloys are frequently employed in orthopaedic implant applications. It is necessary to maximize their general characteristics, corrosion resistance, and ion release. Despite several benefits, coating with torch flame spray has weaker adherence. As a result, powder metallurgy was employed to combine Si and Nb elements with CoCr alloys. CoCrNb and CoCrSi alloys were sprayed with multiple torch flames to apply two different kinds of Nano-coatings (A: 75% HAP+ 25% SiC, and B: 75% Zeolite+ 25% ZrO_2). In two samples, alloying elements Nb and Si were added at a concentration of 5 wt.%. Various characterization methods are employed, such as field emission scanning electron microscopy (FESEM) or energy dispersive X-ray spectroscopy (EDS), an ion release test, atomic absorption spectroscopy (AAS), a wear test, corrosion measurement, atomic force microscopy (AFM), and an adhesion strength test. According to the results, coating (type A) and (type B) increase the wear resistance of CoCr alloy. The zeolite+ZrO_2 (type B) and HAP+SiC (type A) coating layers act as barriers to the release of Co and Cr ions from CoCr alloys. There were varying degrees of roughness in the coated samples, which resulted in corrosion pitting. According to tensile pull-out tests, the two-torch flame spraying technique provided a stronger bond with the substrate than the single-torch flame spraying technique. In general, CoCrSi coated type B are the best to be implanted where the cytotoxicity is 0% in the human body, thus an excellent biocompatibility.

1. Introduction

Stainless steel 316L, titanium, and cobalt-based metal alloys are widely used as orthopedic implants due to its increased mechanical strength, wear stability, and corrosion resistance. All of these metals or alloys, on the other hand, are considered physiologically inert materials [1,2]. These implants are used to stabilize the bones and induce osseointegration with bone tissue [3]. Yet, wear and tear lead to emit potentially hazardous Co, Cr ions. As a result, it should be avoided to inhibit implant failure [1,2].

The coating implants is thought to be a viable approach for improving implant-tissue interactions and promoting biocompatibility and biofuctionality without changing the material's characteristics [4,5]. Since HAP is a major component of bones and teeth, it is frequently employed in biological applications [3]. In vivo, HAP may create a direct chemical interaction with bone [4]. Nevertheless, the fundamental disadvantage of HA is its low mechanical strength, which renders it unsuitable for load-bearing applications.

The biomaterials with high biocompatibility and bioactivity that compensate for limited mechanical strength. It has been observed that silica-based compounds improve bone tissue repair more than HAP alone [6,7]. Moreover, silicate-based materials can direct the formation and evolution of a bone-like apatite layer in simulated bodily fluids (SBF) [8, 9]. Another appealing method of creating harder HAP is to employ 80%HAP-ZrO_2 composites, in which the apatite phase provides biocompatibility

http://doi.org/10.30684/etj.2023.138886.1410
Received 16 March 2023; Accepted 24 April 2023; Available online 25 June 2023
2412-0758/University of Technology-Iraq, Baghdad, Iraq

and bioactivity while the zirconia oxide phase provides high strength [10]. ZrO_2 has been used in orthopedic applications such as hip and knee joints due to its strong biocompatibility and high mechanical qualities [11].

The diverse behaviors of Zeolite-based ceramic composites have been greatly improved [12,13]. Titania reinforced zeolite composite may effectively adsorb polar molecules, as proven by Yasumori et al [13]. Moreover, several studies [14,15] have indicated an improvement in mechanical characteristics in zeolite reinforced ceramic composites. Mechanical activation and reactive sintering were used to create 90-50% zeolite-reinforced alumina composite materials. The composition percentages and temperatures have a significant impact on the qualities of the final goods.

Creating a 90% HAP composite coating is a novel approach to improving mechanical characteristics and corrosion resistance [16]. The SiC biocompatibility and non-toxicity have been demonstrated, and it has been stated that SiC particles do not inhibit bone formation when utilized in coatings applied to medical implants [17]. Hosseini et al.[18] demonstrated that various HAP coatings were produced on AISI 316L stainless steel using a two-step electrophoretic deposition process. The HAP composite coatings were found to be intact and crack-free. HAP-SiC coating was discovered to be an optimal coating sample based on coating morphology. Corrosion tests revealed that a composite covering might increase the corrosion resistance of the SBF implant.

Among coating processes, flame spray coating is a process that melts coating powder using an oxygen flame, producing a porous and composite coating on metallic surfaces. Although the flame spray process is the most economical, deposit efficiency is a high, most widely accepted method of depositing high melting coatings for wear resistance; the flame spray is cold process eliminates damage, metallurgical changes, and deformation to substrate material, and increases equipment portability, components with complicated shape can be coated more readily with manual flame spraying [19].

In this study Alloys of CoCr5Nb and CoCr5Si are prepared by powder metallurgy and sprayed with multiple torch flame spray. Composite Nano-coating involved two kinds are (HAP+SiC and Zeolite+ZrO_2). Scanning Electron Microscopy (SEM)/ Energy Dispersive X-ray Spectroscopy (EDS), an ion release test, Atomic Absorption Spectroscopy (AAS), Wear test, Corrosion assessment, Atomic Force Microscopy (AFM), and adhesion strength tests are used to analyze the uncoated and coated CoCr based alloys. The aim of this review is to provide an integrated overview of the current state of composite coating of metallic implants for orthopedic implant material.

2. Experimental part

2.1 Materials Used as Substrates

As substrates for coating, samples of two different CoCr-based alloys, 65Co30Cr5Nb and 65Co30Cr5Si, were employed. These alloys were prepared by powder metallurgy, i.e. mixing, pressing and sintering. First, each sample's powder is compacted using a hydraulic press machine with a punch and dies of 10mm diameter. Next, the powders were subjected to a pressure of 10 tons for 10 minutes at a speed of 1 mm/s. Next, the samples were heated for four hours at rates of 40°C per minute from 0 to 500°C, 5°C per minute from 500°C to 1330°C for CoCrSi, and 1720°C for CoCrNb in a room that had a vacuum environment around it to prevent materials from oxidizing. The mechanical properties of CoCr-based alloys are shown in Table 1.

Table 1: Some of measured Mechanical properties of CoCr based alloys

Alloy properties	Hardness (MPa)	Ultimate Tensile Strength (MPa)	Elastic modulus (GPa)
CoCrNb	4709	87.71	171.4
CoCrSi	4954	95.19	167.8

2.2 Materials Used for Coating

Two Nano-composite coating materials: (75%Hydroxyapatite+25%SiC) and (75%Zeolite+25%ZrO_2) are used as a coating layer; both consist of bioactive and bioinert ceramic—the properties of coating materials as shown in Table 2.

Table 2: General properties of coating materials

Compound properties	Chemical Formula	Origin	Purity	Particle size(nm)
Hydroxyapatite	$Ca_{10}(PO_4)_6(OH)_2$	US Research Nanomaterials, Inc., 3302 Twig Leaflane, Houston, TX77084, USA	>99 %	25
Silicon carbide	Beta SiC	US Research Nanomaterials, Inc., 3302 Twig Leaflane, Houston, TX77084, USA	>99 %	45-65
Zeolite	$Na_nAl_nSi_{96n}O_{192}\cdot 16H_2O$ ($0<n<27$).	US Research Nanomaterials, Inc., 3302 Twig Leaflane, Houston, TX77084, USA	>99 %	50
Zirconia	ZrO_2	US Research Nanomaterials, Inc., 3302 Twig Leaflane, Houston, TX77084, USA	>99 %	20

2.3 Multiple Flame Spray

The sand blasting is used to roughen a sample's surface before flame spray coating. Two torch flame spray coating was carried out. The fuel/oxygen flame is created by mixing gases; the combination goes through a nozzle and ignites to create a high-intensity two-flame. Acetylene at 0.7 pressure, oxygen at 0.5 bar, and 0.85 m^3/min compressed air at 4.5 bar are used in gas combustion.

The gun flame temperature ranges between 2500 and 2700°C. The spray distance is 120 mm at a 90-degree angle. After the powders are fed into the flame, the melted ceramic coating is formed. The molten ceramic is subsequently atomized and projected onto the substrate.

2.4 Characterization Techniques

The following tests were performed to evaluate the samples performance:

2.4.1 FESEM and EDS

The prepared samples before and after coating (10mm Diameter, 5mm Height) were examined using SEM (MIRA3 by TESCAN Co., Czech Republic origin) (high-energy electrons beam in a raster scan pattern).

An Energy dispersive analysis (EDX) is used to determine the chemical composition of the material. The results of an EDX examination are spectra with peaks corresponding to the substance's components being studied [20].

The prepared specimen's surfaces were firstly grounded with SiC paper up to a 3000 grit level and then polished with an alumina powder of 5µm grain size. Following that, the prepared samples' surfaces were subjected to scanning.

2.4.2 AFM

An essential technology for measuring surface roughness by Atomic Force Microscopy is the evaluation technique for the shape of AFM tip. Evaluation of the AFM tip's profile using a probe inspection sample. The surface roughness and texture of the device components have a direct impact on the overall performance and quality in the majority of applications. The characterization was done by NaioAFM Nanosurf Switzerland.

2.4.3 AAS

Since the samples, except the face, were covered with epoxy, there was slight relative motion between them and the corrosive solution. A material that simulates biofluids was added to each sample's container. It was a ringer solution. The samples went through a 37°C water path incubation. The containers are tightly closed to prevent contamination and evaporation of the testing fluid. During the 14-day immersion period, the quantity of solution extracted by syringe for 3,7 and 14 days was used to carry out the ion release. The American-made Varian Spectra AA 220FS determined the kind and quantity of the ions emitted from the metallic implant materials.

2.4.4 Corrosion test

The corrosion rate was determined using a ringer solution as a simulated body fluid (SBF) with pH 6.9 and a voltage between 0.3 and 3 V using a potentiostat (Vertex. One, Netherlands).

The working electrodes were created and tested at 37°C by ASTM G108-94 standard [21]. Tafel curves were made at a rate of 1 mv/sec to calculate the current density and data collection rate: 300kHz; compliance: 100mA/21V; applied scan range: 10V; current ranges: 100pA-100mA; minimum resolution: 3fA. The measurement of the corrosion rate was obtained by using Equation 1 [22].

$$Corrosion\ rate\ (mpy)\ =\ (0.13\ icorr\ (E.W.))\ /\ A \quad (1)$$

mpy: mils per year, icorr: corrosion current, E: equivalent weight, A: area

2.4.5 Wear test

ASTM G99-05 was followed for conducting the wear tests. The dimensions of cylinder samples were 10mm in diameter and 25mm in height and loaded perpendicular to the desk [23].

$$Wear\ rate\ (g/cm\ ) = \Delta W/SD \quad (2)$$

$$\Delta W = W1 - W2 \quad (3)$$

ΔW(gram): the difference in the mass of samples prior (W1) to and after (W2) the test.

SD: distance Slide (SD) (cm), is calculated from the following relationship:

$$SD = 2\pi\ n\ t\ r \quad (4)$$

where r= 8cm (radius of sample to disc's center), n= 375 rpm (number of disk sessions), t=5min (test period), load = 500g.

2.4.6 Tensile pull-out adhesion test

The test usually involves coating a cylindrical specimen's face with a thermal spray before attaching the beginning of an identical uncoated sample to the coated surface using high-strength cyanoacrylate (super glue). The coating's tensile strength is calculated by dividing the highest load at failure by cross-sectional area [24].

The bond strength is provided if the failure occurs at substrate - coating interface. The cohesive strength of the coating is evaluated if the failure entirely occurs within the layer. The adhesive will not endure the superior coatings. When this method determines the adhesive's tensile strength, the result is an upper bond strength [24].

The sample has a 10mm diameter and 20mm height in dimensions. The tests were performed on three samples, and the results were documented.

2.4.7 MTT assay

In order to determine the survival rate of human osteoblast-like cells (MG63) treated with 12 nanoparticles uncoated and coated samples and to determine cytotoxicity, these compounds were examined by the MTT method. The steps are as follows carried out by Shahrood University of Technology/Iran.

1) Human osteoblast-like cells (MG63) cells with a concentration of 10^4 cells per 100 microliters were cultured in DMEM and RPMI complete culture medium in a 96-well plate and incubated in an incubator at a temperature of 37°C. The studied groups include the control group, the treatment group with nanoparticles uncoated and coated samples.
2) After 24 hours of incubation, the cell groups related to the treatment were treated with a 100 µl of nanoparticles. They were treated and incubated in an incubator for 24 hours.
3) In order to prevent the absorption error that the nanoparticles may cause at the end of the experiment, 6 wells containing only the culture medium and each of the nanoparticles were allocated.
4) After 24 hours of treatment, the drug along with the medium was removed from all the wells and MTT was added to the cells at a ratio of 1:5 with the culture medium and they were incubated for 4 hours in the incubator. (Each well contains 20 µl of MTT and 80 µl of culture medium)
5) After 4 hours, the medium with MTT was carefully removed from the wells, and the formed MTT crystals were dissolved by a 50 µl of DMSO.
6) The absorbance of MTT was measured by 630 nm wavelength by eliminator or plate reader.
7) Experiments were repeated three times.
8) Calculation of cell viability:

$$\text{Calculation of cell viability\%} = \frac{Mean\ OD\ sample}{Mean\ OD\ blank} \times 100 = \text{survival rate\%} \quad (5)$$

$$\text{Cytotoxicity rate} = 100 - \text{Survival rate} \quad (6)$$

3. Results and Discussion

3.1 FESEM and EDS

Field Emission Scanning Electron Microscope was carried out on all implant samples. They were utilized to make appropriate observations of the surface topography and to detect the influence of the coating on the surface textures of the implants. The samples were sprayed with Nanocomposite coating, and the coating thickness observed ranged from (150-170 µm), as shown in Figure 1 (a,b).

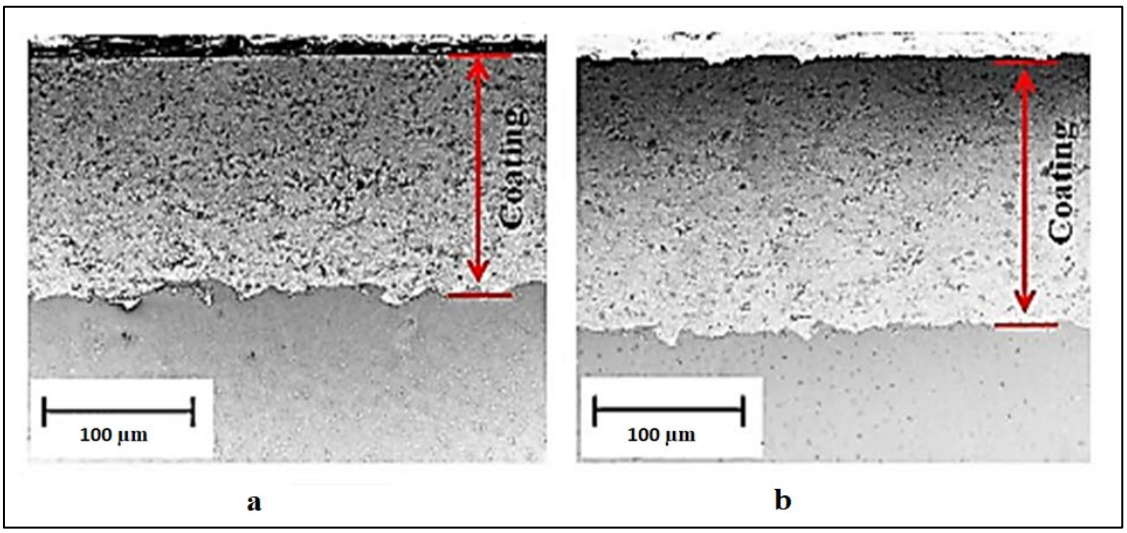

Figure 1: (a,b) Coating thickness of the coated samples by flame spray

The microstructure observations of samples in Figures (2a, 3a, 4a, 5a, 6a and 7a) reveal that coating was homogeneously dispersed and completely covered the surface, resulting in a considerable change in surface morphologies as a result of surface roughness caused by the manufacturing process (powder technology) and the primary surface treatment (sand blasting) performed prior to the coating process to prepare the surface for coating. Using primary surface treatment and powder technology proved advantageous and successful in producing a homogeneous and adhered coating layer.

Energy dispersive spectroscopy (EDS) was used to perform elemental analysis or surface chemical characterization of such a sample before and after coating. This test was performed to determine the influence of the coating on the implant surface chemistry due to the precipitation of some elements on the surface caused by surface coating. The surface chemical analysis reveals a significant peak of cobalt, chromium, Silicon, and niobium without any other

Peaks of elements, indicating that the samples are of high purity and the production process does not affect or result in a change in the surface chemical composition as shown in Figure (2b and 3b). However, the flame spray technique significantly changed the surface chemical composition of coated samples after covering the surface with composite coating as in Figure (4b, 5b, 6b, and 7b). In addition, a high percentage silicon peak was seen in all group samples, indicating the precipitation of coating layer SiC in type A coating and Si in zeolite of type B coating.

The hydroxyapatite phase illustrated in the light region and the SiC phase with a little matrix (CoCrNb, and CoCrSi) according to substrate alloy in the dark area of Figure (2a and 3a), respectively. The Hydroxyapatite phase was 75%, and the SiC phase was 25% (2b and 3b) detected by (EDX) detector. The morphology was characteristic of an irregular kind. The coating contained porosity, as illustrated in (4a and 5a), because the layer has a high percentage of HAP, which enhances Osseointegration.

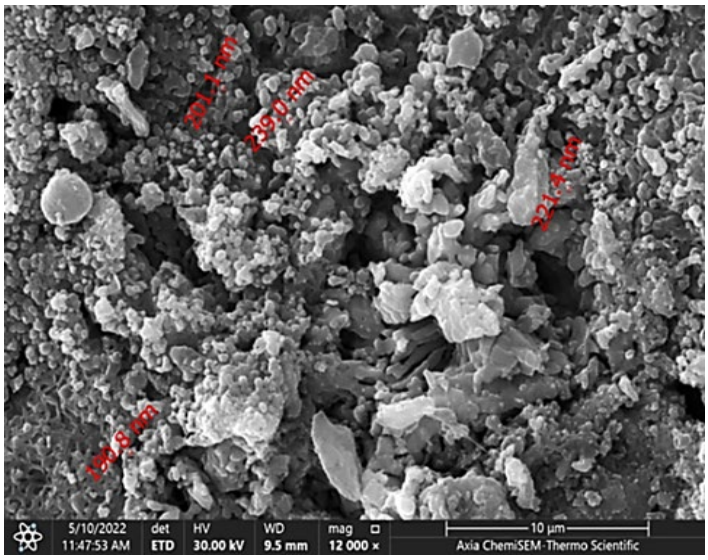

(a)

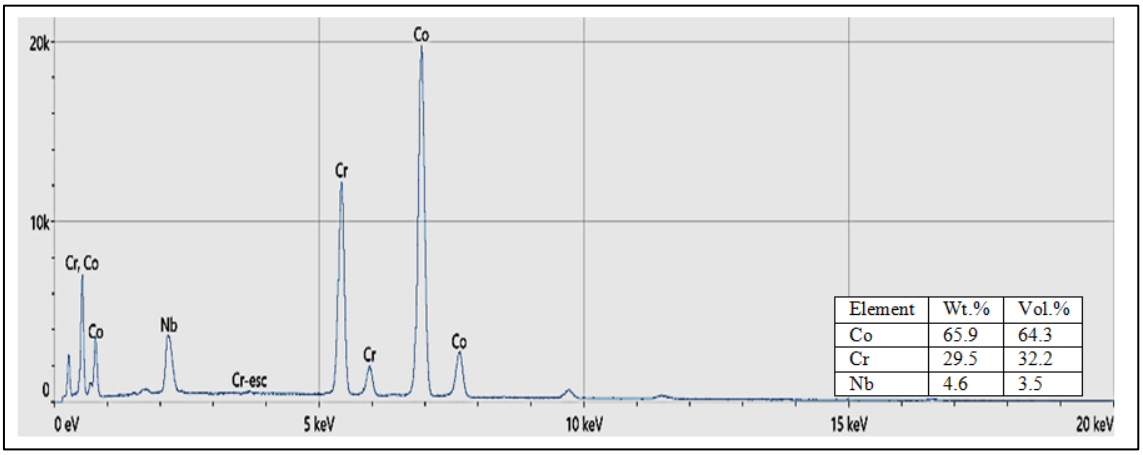

(b)

Figure 2: (a,b)FESEM and EDS of CoCrNb alloy prepared by powder metallurgy

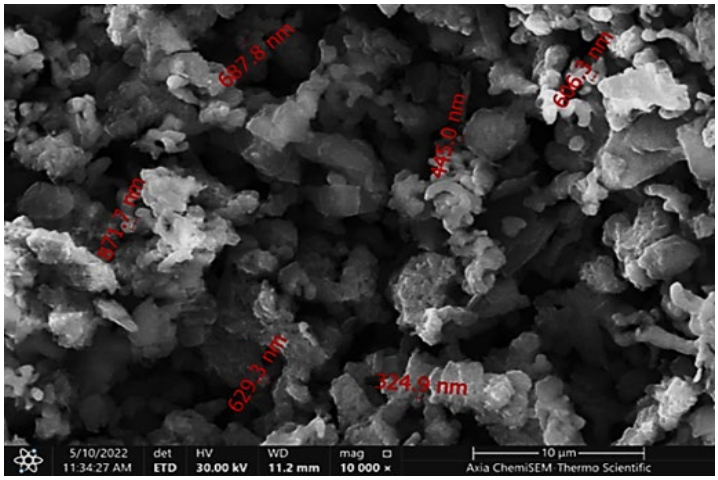

(a)

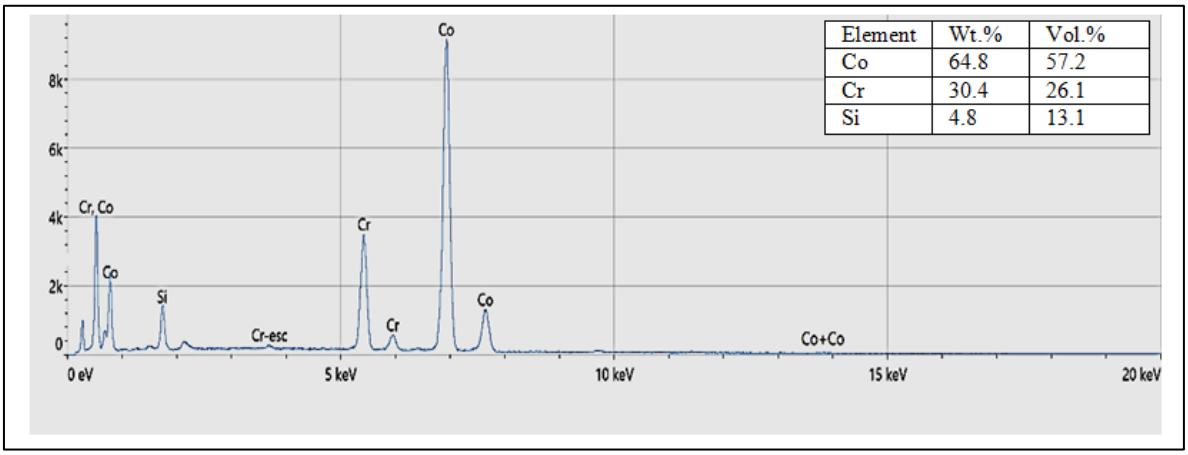

(b)

Figure 3: (a,b) FESEM and EDS of CoCrSi alloy prepared by powder metallurgy

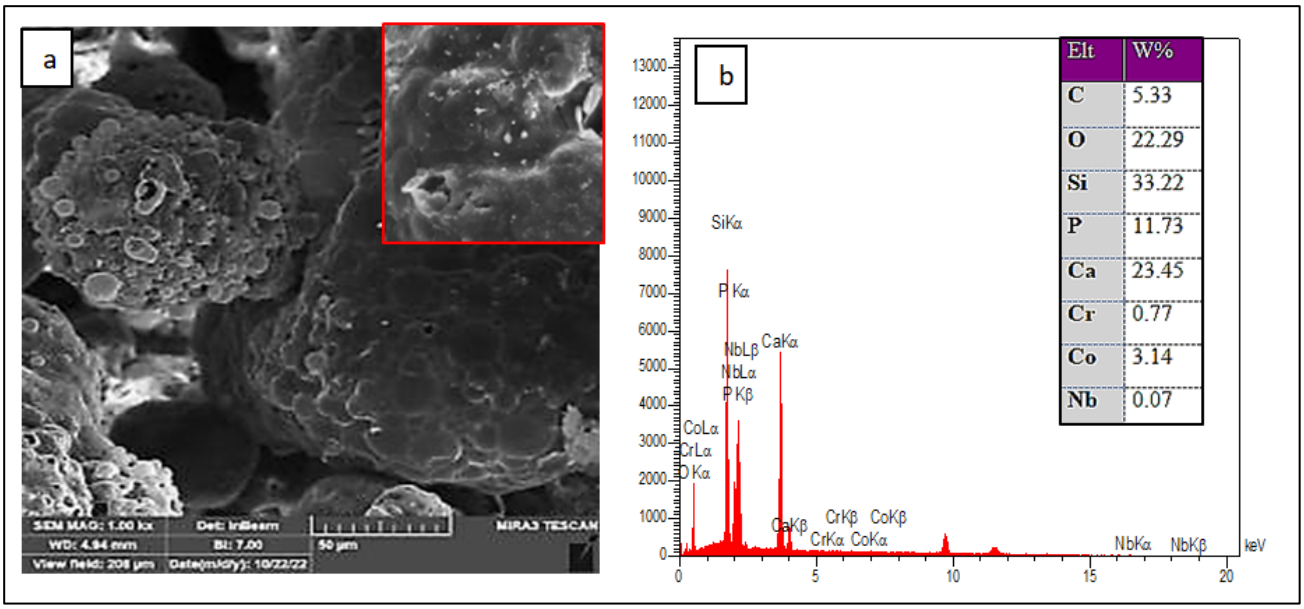

Figure 4: (a,b) FESEM and EDS CoCrNb coated with 75% HAP + 25% SiC (type A)

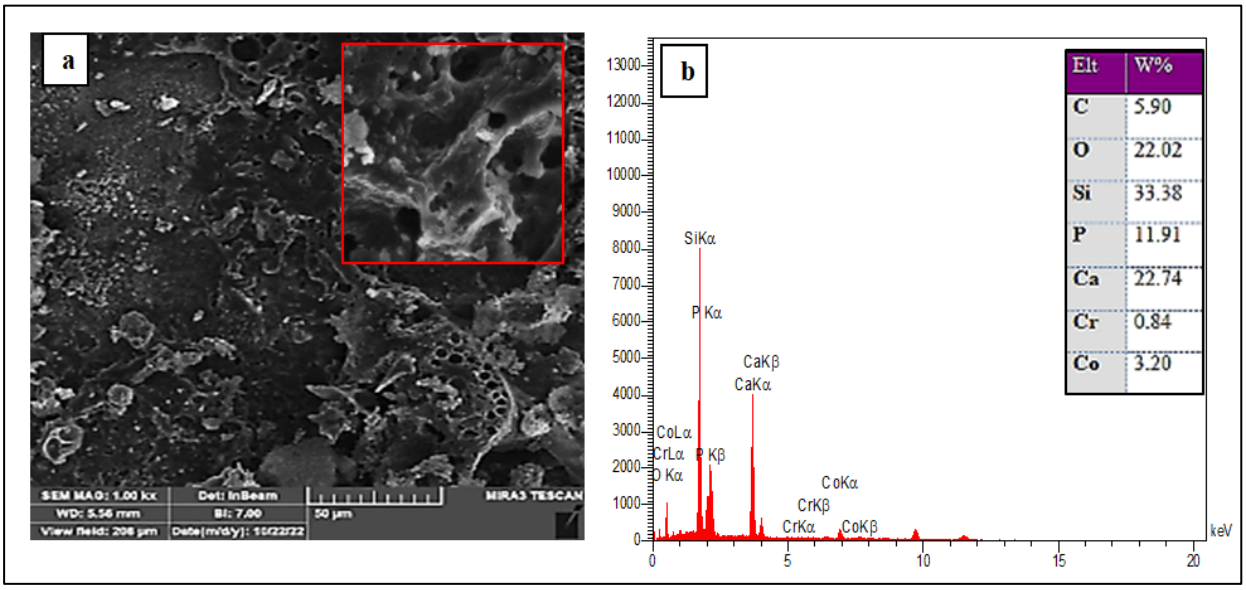

Figure 5: (a,b) FESEM and EDS CoCrSi coated with 75% HAP + 25% SiC (type A)

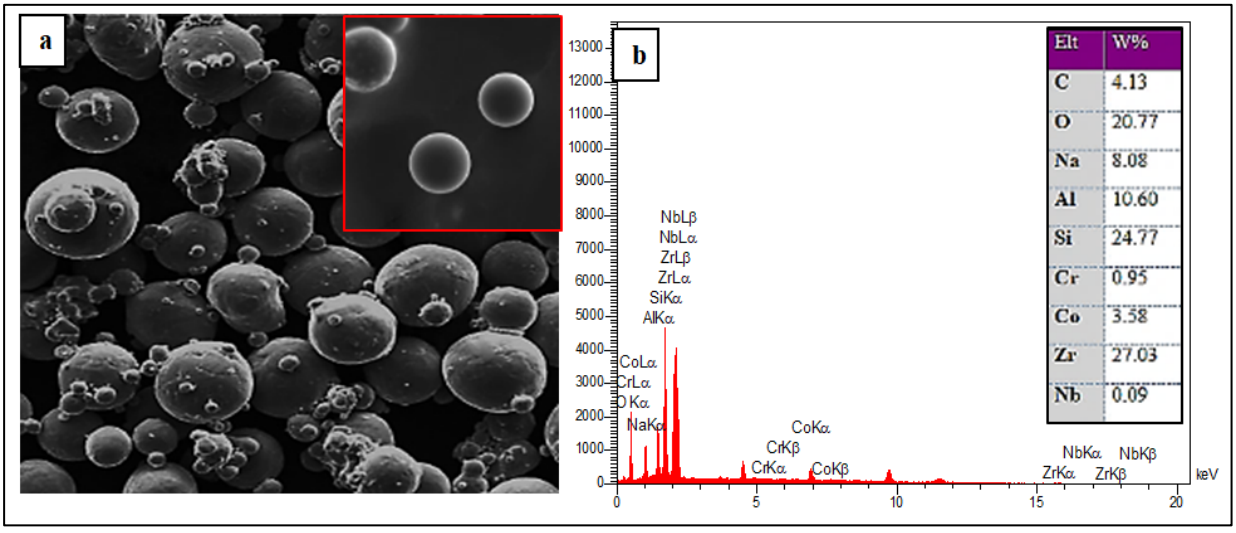

Figure 6: (a,b) FESEM and EDS of CoCrNb coated with 75%Zeolite+25%ZrO_2(type B)

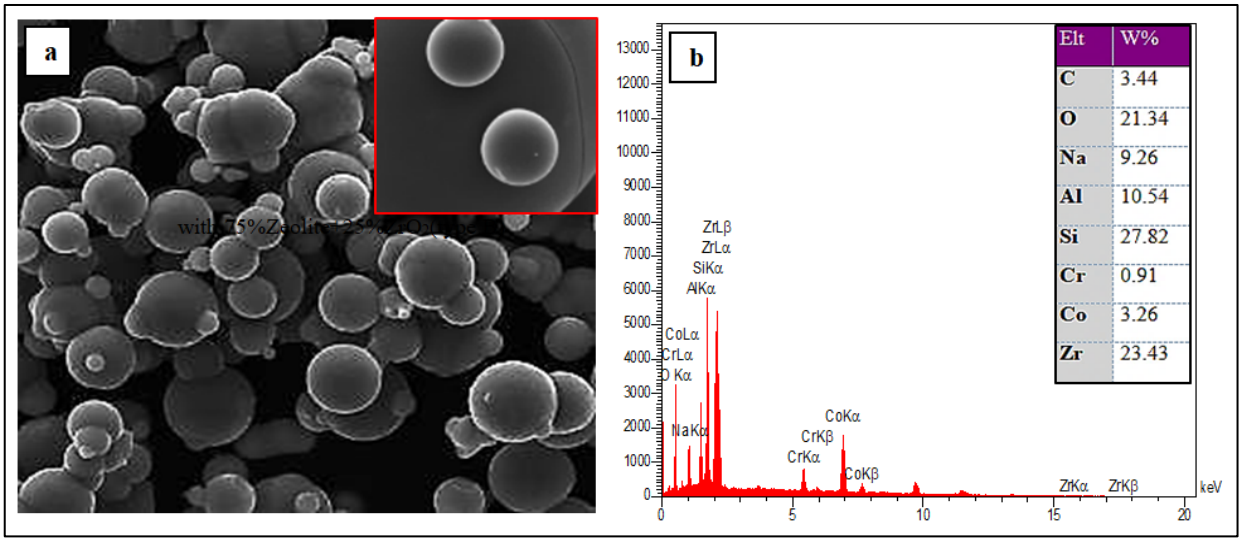

Figure 7: (a,b) FESEM and EDS of CoCrSi coated with 75% Zeolite+25% ZrO_2 (type B)

ZSM-5 Zeolite and zirconia phases are shown as balls in the matrix (dark area) in figures (6a and 7a), according to the substrate alloy of CoCrNb, and CoCrSi, respectively. The (EDX) detector identified the (6b, 7b) ZSM5 Zeolite phase (75%) and

the Zirconia phase (25%). The morphology was typical of a circular kind. No porosity is present in the coating, as shown in Figure (6a and 7a), because a significant portion of the layer is nonporous.

3.2 Atomic Force Microscopy AFM

Surface roughness has been found as a significant feature for implant anchoring capability in bone tissue. The most often utilized procedures for increasing the implant's surface roughness include sand blasting, coating, or a combination of these.

Atomic-force microscopy (AFM) was used to show the surface topography, which produced an image of the three-dimensional form (topography) of a sample surface at a high resolution. This is accomplished by scanning the sample's location relative to the tip and measuring the probe's height, corresponding to a fixed probe-sample contact [25].

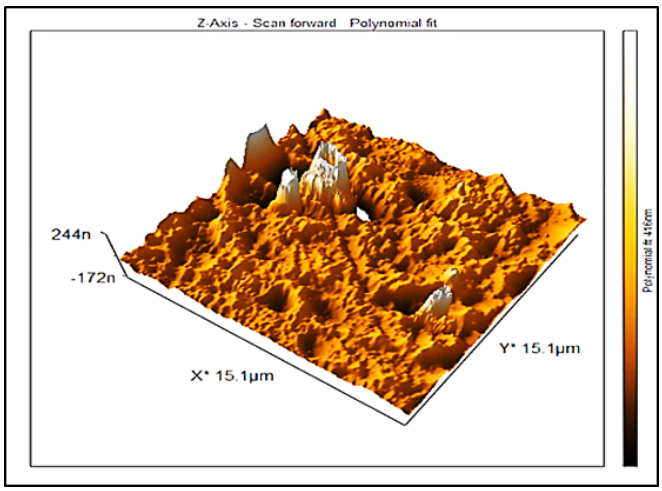

A- For samples coated A(HAP+SiC)

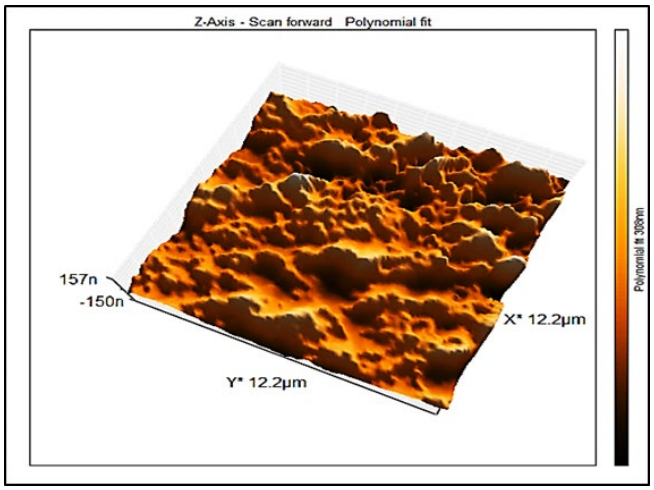

B- For samples coated B (Zeolite+ZrO_2)

Figure 8: (A,B)Surface topography and roughness of all samples with various parameters

The examination results of AFM showed a surface image of the samples, as in Figure 8 (a,b) as well as the mean square root and surface roughness, as indicated in Table 3. The square root mean is denoted by Rq, while Ra represents the surface roughness value.

All the coatings exhibited a substantial waviness/roughness due to flame spraying. Samples have high degrees of roughness since the implant samples were blasted with SiO_2 particles before coating; the surface roughness and morphology increased significantly due to a fine superficial layer, and the coating formed a fibrous texture on the implant surface ranging from nano to micro size. The different sizes of top-layer particles that are not deformed are another cause of increased roughness. HAP+SiC and Zeolite+ZrO_2 coating measurement profiles are shown in Figure 8. The roughness values (Ra) attained for each coating are shown in Table 3. the coatings HAP+SiC and Zeolite+ZrO_2 are roughly the same in texture. There was no smooth melted surface to be seen for flame spray; then corrosion pitting will occur by significant roughness because of the high-stress concentrations at rough positions [25].

Table 3: Roughness and Square root mean values

Samples	Surface roughness value (Ra nm)	Square root mean (Rq nm)
Samples coated A(HAP+SiC)	91.85	139.8
Samples coated B(Zeolite+ZrO_2)	81.70	116.4

3.3 Atomic Absorption Spectroscopy (AAS)

As a direct result of the corrosion process, ions are liberated from implant materials. Metal ion release can cause local and systemic health concerns owing to ion diffusion throughout the body. Therefore, the number of ions liberated from all groups of implant samples in the Ringer solution was determined.

Low concentrations of dissolved oxygen, inorganic ions, proteins, and cells may accelerate metal ion release. The electrochemical rule governs the behaviour of metal ions released into biofluid. The released metal ions do not always combine with biomolecules to cause toxicity. The active ions immediately combine with a water molecule or an anion nearby to form an oxide, hydroxide, or inorganic salt. As a result, there is only a minuscule probability that the ion will mix with biomolecules and produce cytotoxicity, which was not detected in the present sample [26].

The coating films on implants were discovered to be crucial ion-release inhibitors. From Figures (9 and 10), it can be seen that the ion release increases within 3–7 days and then start to stabilize. This resulted from ions migrating from the surface when metal is dissolved inside a body due to adsorption [26].

As immersion time rises, more ions are released until adsorption-desorption equilibrium is reached, where the number of released ions will be constant. Simultaneously, these ions will interact with molecules in the environment and carry away on other surfaces .

Furthermore, a study on cellular processes at the implant-bone contact discovered that several responses occur at the implant's surface when the implant is put into the body. The processes, known as serum adsorption, occur soon after the implant is introduced and involve the response of the implant surface with protein, carbohydrates, liquids, and mineral ions. After three days, another response (mesenchymal cell requirement) begins. This means the metal ion adsorption was fixed by creating cells at the surface, which can operate as ion release prevention [27]. Figure 9 show CoCrNb has higher Co ion release and CoCrSi coated zeolite+ZrO_2 has deficient Co ion release.

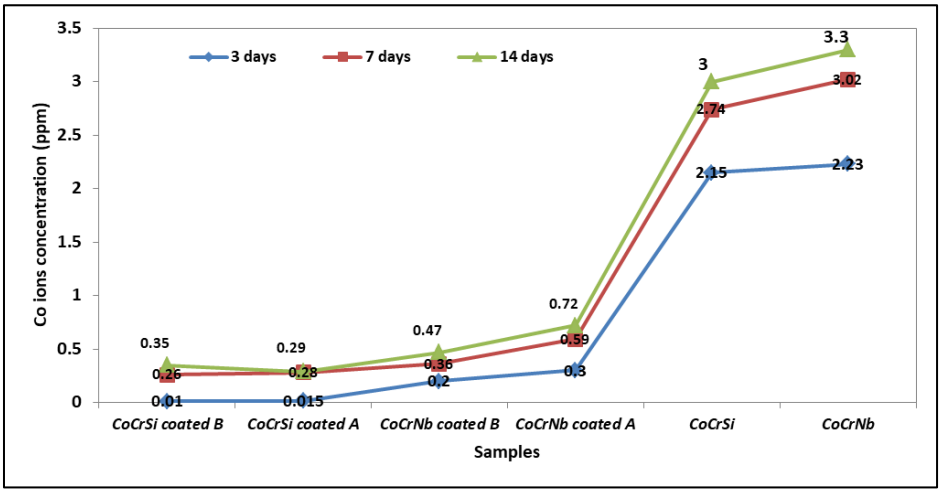

Figure 9: Cobalt ions release of base (CoCr) and coated alloys by two torch flame spray

Figure 10 show that coated CoCr alloy has no Cr ion release while uncoated CoCrNb and CoCrSi have Cr ion release.

Blasting with SiO_2 particles improved surface characteristics by forming a work-hardened superficial layer, in addition to the secondary treatment that prevents ion release. Zeolite+ZrO_2 (B) and HAP+SiC (A) acts as a barrier to inhibit the release of Co and Cr ions for CoCr alloys. Differences in ion number released from samples were caused by either a primary or secondary surface activation method, which altered the stability and thickness of the oxide layer [28].

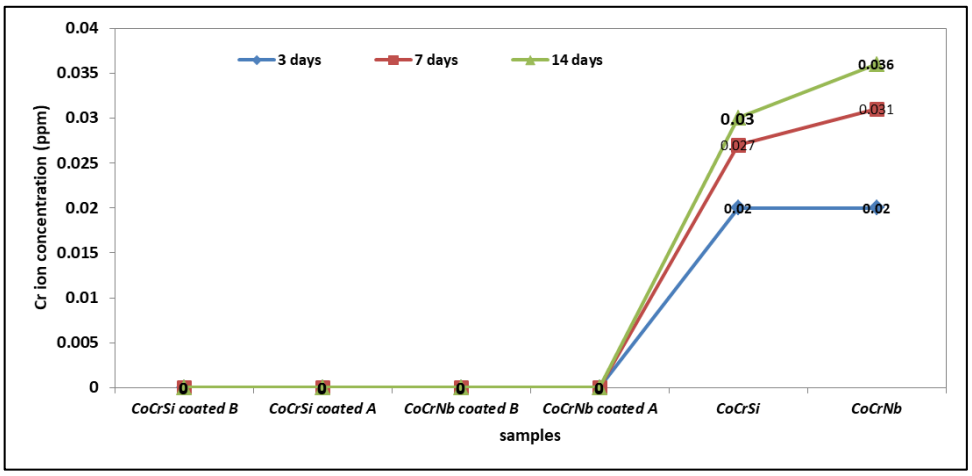

Figure 10: Chromium ions release of base (CoCr) and coated alloys by two torch flame spray

3.4 Corrosion Test

Potentiostatic polarization was accomplished using the potentiostatic polarization test in Ringer solution for uncoated and coated samples at 37°C. Polarization curves of A, B coated samples are given in Figure 11a-f. Table 4 shows the corrosion parameters (corrosion potential, corrosion current, and corrosion rate) retrieved from tafel curves.

Table 4: I corr and Ecorr of samples used

No.	Sample	T (K)	Ecorr (mV)	Icorr (mA/cm^2)	C.R (mm/y)
a	CoCrNb	313	-557.2	0.07151	0.8306
b	CoCrSi	313	-541.6	0.06624	0.537
c	A coated CoCrNb	313	-502.4	0.05522	0.18070
d	A coated CoCrSi	313	-220.2	0.00896	0.0293
e	B coated CoCrNb	313	-50.00	0.01630	0.05334
f	B coated CoCrSi	313	130.1	0.00564	0.01638

Compared to uncoated samples, the corrosion potential of all coated samples shifts significantly to the positive side and has a higher noble potential. Furthermore, the (c, d, e and f) samples have substantially lower current densities and corrosion rates than uncoated samples (a and b), indicating that ceramic coating functions as a barrier against aggressive ion attack, significantly improving the corrosion resistance of CoCr alloy implant. Because of the reduction in iron released from the metal surface, the corrosion ratio for the implant within people's bodies can be minimized by coating the sample with bioactive HAP or Zeolite. However, HAP and Zeolite possess favoured properties, leading to their widespread use in implant protection. Contact between the tissue surrounding the bones and the metal prosthesis is one of the implantation procedures needed for prostheses. The availability of HAP and Zeolite in coating for the implant will result in quick bonding between the tissue around the bones and the metal prosthesis [29].

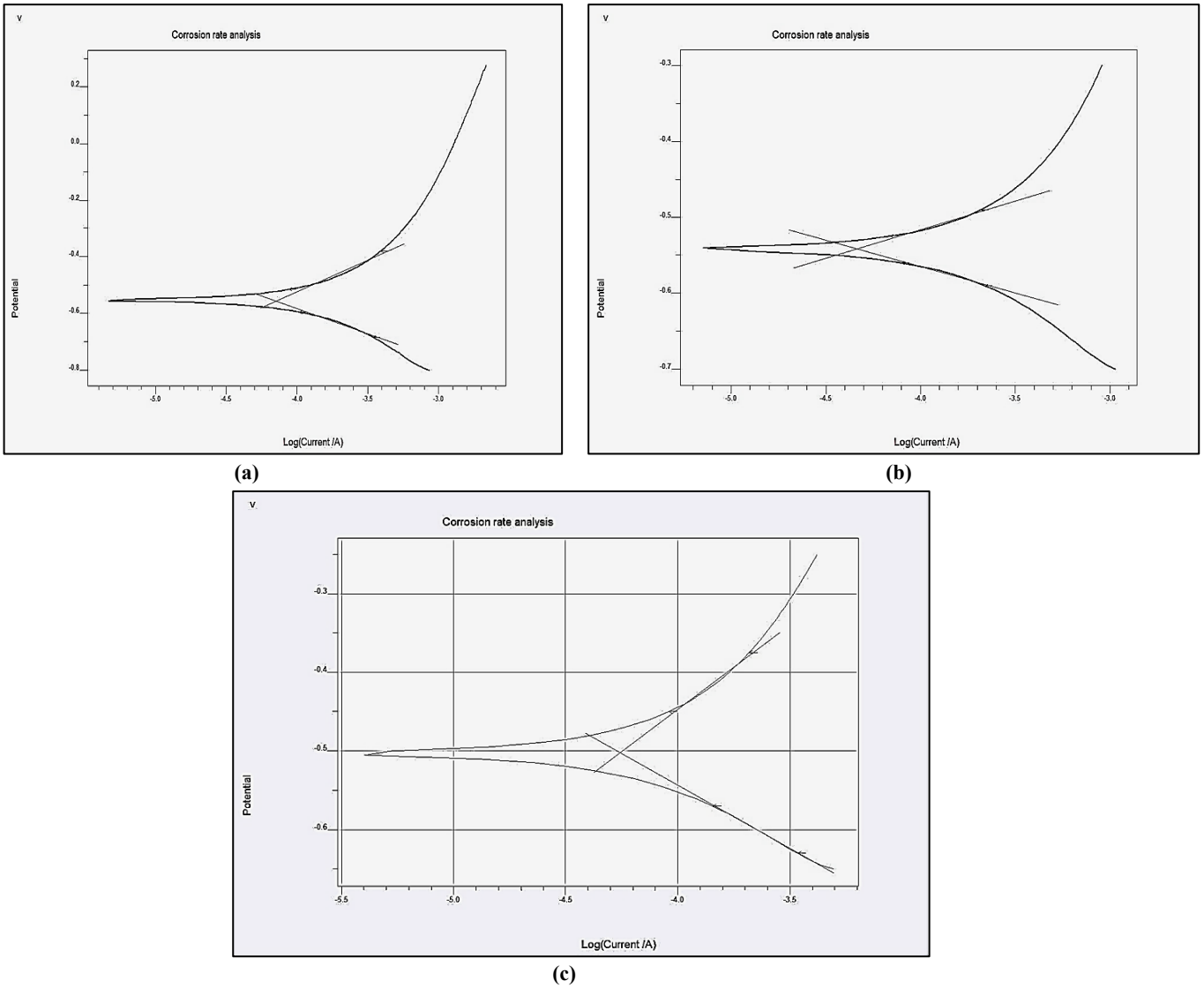

Figure 11: (a,b)Tafel curves of the samples. (a) A coated samples, (b): B coated samples(c,d,e,f) Tafel curves of the samples, (c):A coated CoCrNb, (d):A coated CoCrSi, (e):B coated CoCrNb, (f):B coated CoCrSi

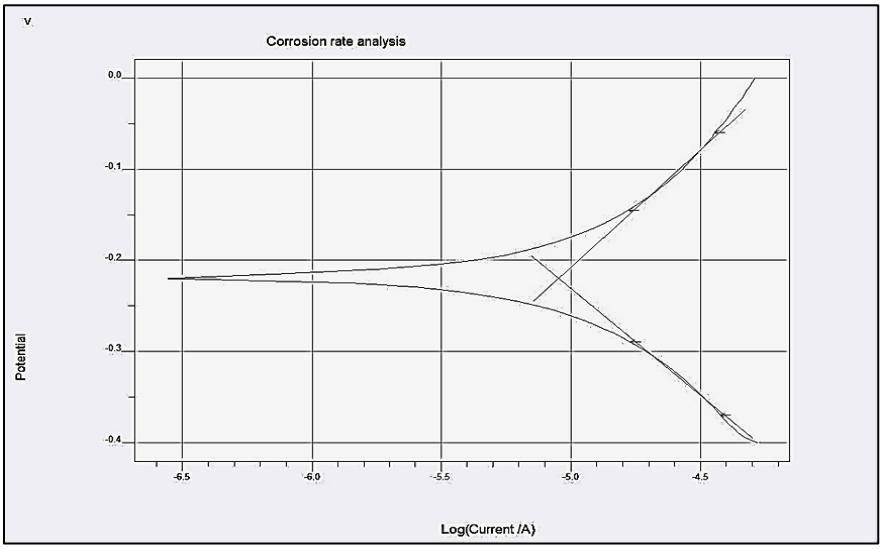

(d)

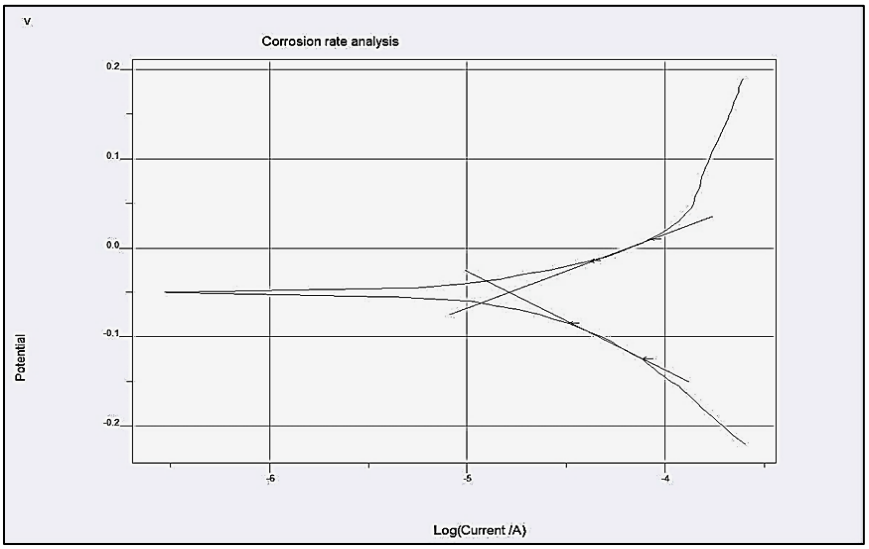

(e)

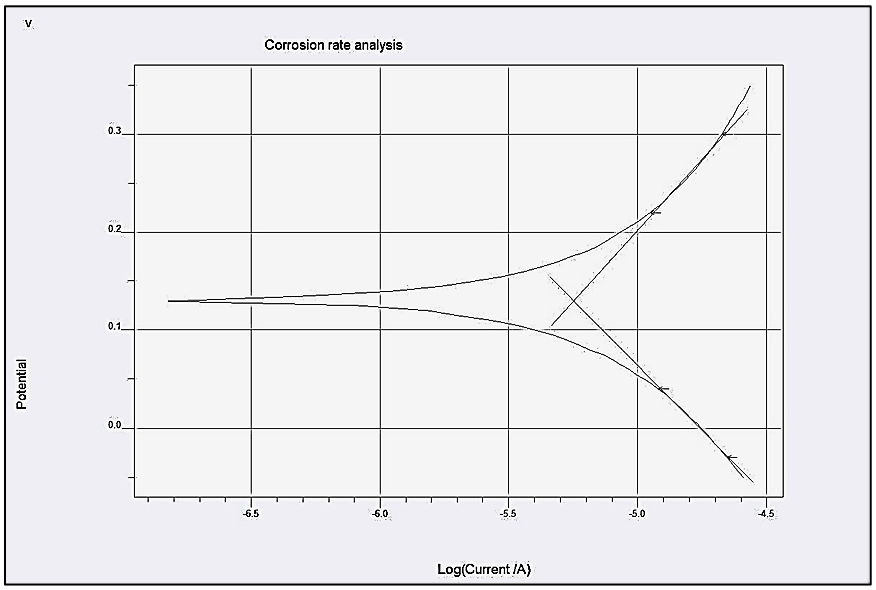

(f)

Figure 11: Continued

Numerous factors contribute to composite coating usage, consisting of bioactive (HAP, Zeolite) and bioinert (SiC , ZrO_2) in covering implants. Since HAP and zeolite is a biocompatible substance, bioinert (SiC and ZrO_2) have strength, wear resistance and biocompatibility; the bioactive substances in large ratio leads to ingrowths of bone and tissue surrounding it, as well as chemical processes that promote bonding. Moreover, HAP or zeolite (75%) in implant metal coatings increases the metal resistance to corrode when soaked in Ringer solutions by strengthening chemical bonding and decreasing metal iron release .

The substrate and the corrosive environment are separated by a passivation coating, which improves corrosion resistance. The passivation coating becomes more compact and complete as the silicon percentage increases, and the alloy's corrosion resistance improves; thus CoCrNb had higher corrosion rate values than CoCrSi. However, due to the coating composition of type B (alumina, silica), and zirconia has the most robust corrosion resistance because of their highly protective oxides and chemical inertness, CoCrSi coated Zeolite ZSM5 plus ZrO_2 (f) corroded at a minimal rate.

3.5 Wear Test

Thermal spraying is frequently considered a viable alternative to typical coating manufacturing procedures for creating wear-resistant coatings. Ceramic thermally sprayed coatings, in particular, have been used for anti-wear applications. In addition, flame-sprayed coatings are commonly utilized to extend the service life of wear-prone items [30].

The wear rate of the uncoated samples was approximately constant, while that of the coated samples continued to fall but at an approximately reduced rate. There was a heavy fluctuation in the friction coefficient values for the uncoated sample compared with the coated samples. As presented in Table 5, the uncoated samples exhibited twice a higher wear rate than the coated samples .

CoCr alloys generally have a higher wear rate, as in Figure 12, because they have excellent hardness compared with other joint implant alloys. For base samples, CoCrSi has a low wear rate. For coated samples, CoCrSi coated with HAP+SiC has higher wear resistance than the different samples used.

According to the test findings, Zeolite+ZrO_2 (type B) sprayed coatings had more excellent wear resistance than HAP+SiC (type A) coatings, and the higher the content, the lower the wear rate. The Coating surface roughness usually is high, and due to sliding, the rough surface asperities smoothen, which in turn increases the contact area that is directly linked to an increase in wear. The higher value of Roughness will lead to the ploughing of asperities on the coating surface.

Table 5: ΔW values of samples

No.	ΔW (Base)	ΔW (Coated HAP+SiC)	ΔW (Coated Zeolite+ZrO_2)
CoCrNb	5.30E-03	3.52E-03	2.72E-03
CoCrSi	2.50E-03	1.82E-03	1.42E-03

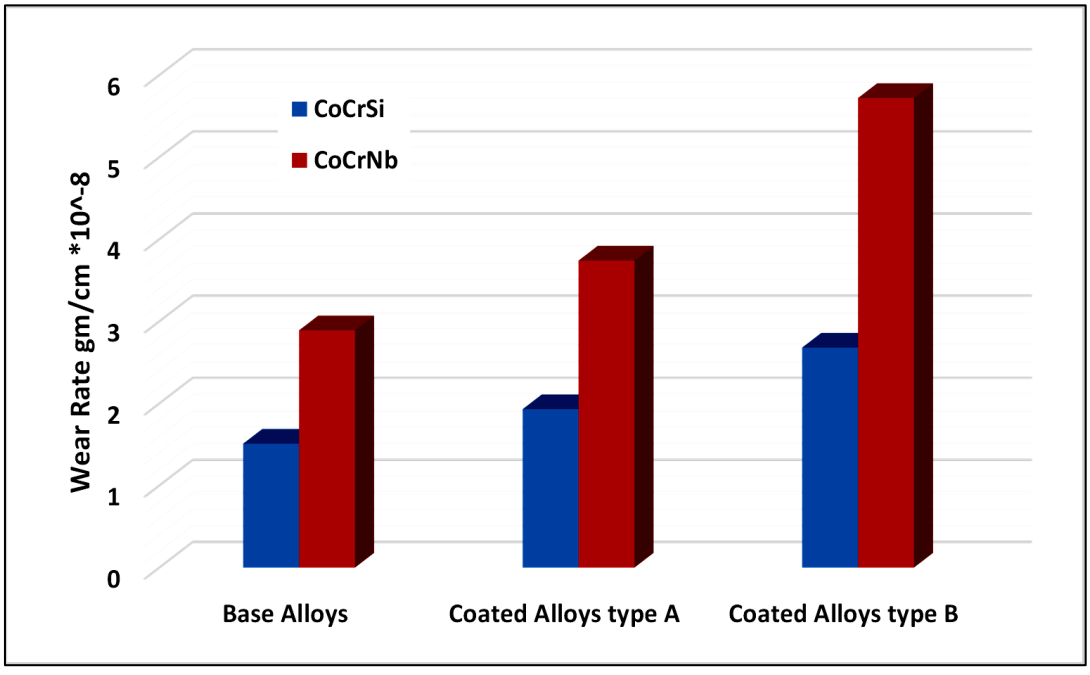

Figure 12: Wear rate of base (CoCr) and coated alloys by flame spray at 500gram for 5min

3.6 Tensile Pull-off Adhesion Test

As in Figure 13, the results showed pull-off strength ranging between 24-26 MPa, which refers to the tensile strength of cyanoacrylate (glue) as ~ (27Mpa). When the test is carried out, the glue fails without delamination or in the coating layer. Therefore, these results referred to good adhesive strength of the coating with the substrate; the adhesive strength values of two-torch flame spray are higher than single torch spray .

Generally, multiple torch flame spray led to the increased thickness of the coating; thus, roughness increased. The surface roughness played a significant role in adhesive bonding between the coating with the substrate. For numerous reasons, a rough surface frequently results in stronger bonds:

-Roughness provides more surface area for the adhesive to make contact with while making a connection.

-A rough surface adds mechanical interlocking at the interface. In addition, surface irregularities may reduce fracture propagation, allowing for stronger, more wear-resistant bonding [31].

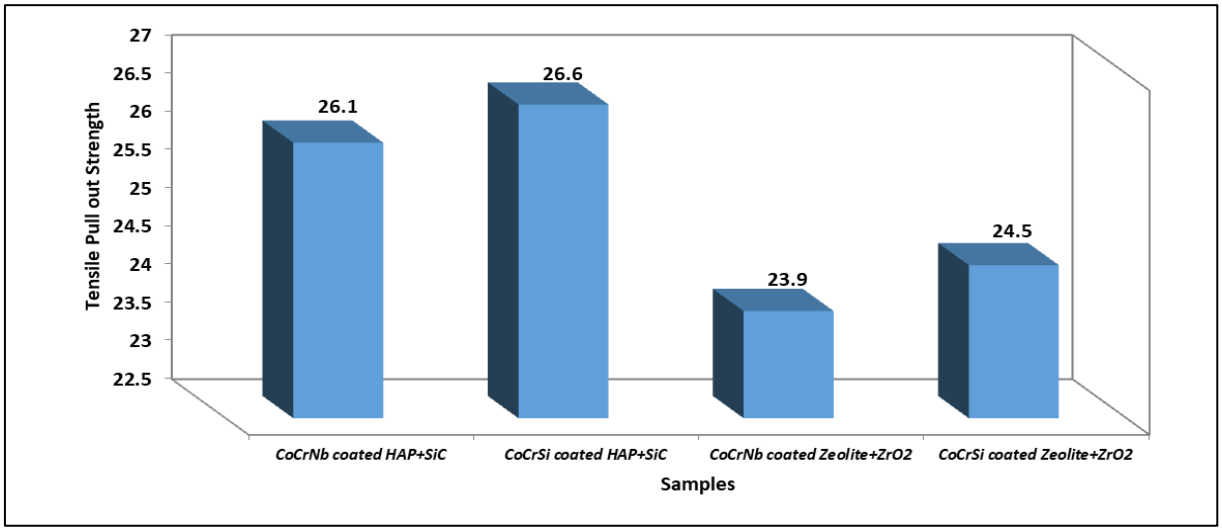

Figure 13: Tensile pull-out strength of Coated alloys with HAP+SiC (A) and Zeolite+ZrO_2 (B) by two torch flame spray

3.7 MTT Assay

An implant's surface must be non-toxic and non-irritating to neighboring biological tissues. A cytotoxic test was performed as a biological evaluation of the implant created to fulfill this criteria.

The indirect cytotoxicity experiments revealed that the alloy extracts do not impair osteoblast cell growth, with the number of viable cells being comparable to or greater than 85% (no toxicity) [32]. When incubated with viable cells, the MTT reagent is reduced to a DMSO product, and the absorbance of DMSO indirectly reflects the amount of cell viability in the culture.

The amount of live MG63 cells adhering to the sample surface is shown in Figure 14. Cell adhesion to the coated surface was dramatically increased after 24 hour of culture as compared to the other samples. Cell adhesion on the surface of CoCrNb less than all other samples at all time period.

Moreover, CoCrSi coated B has no cytotoxicity as in Figure 15, Because of inhibition release of Co and Cr ions by formation adherence protective film consist of alumina, silica and Zirconia, they are very biocompatible for human body.

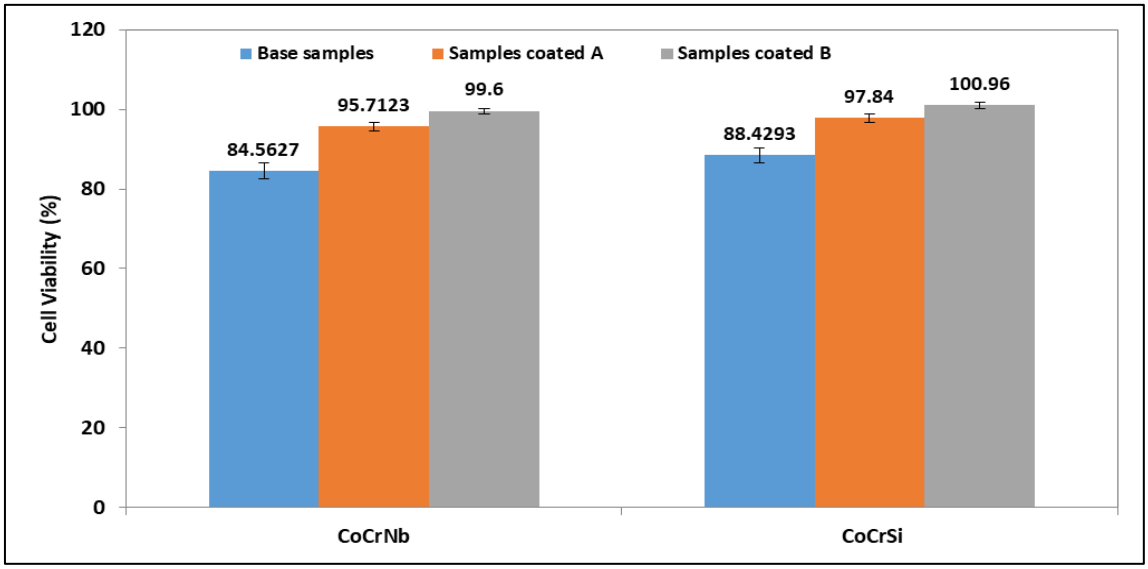

Figure 14: Cell viability of the base (CoCr) and coated samples by two torch flame spray with HAP+SiC (A) and Zeolite+ZrO_2 (B) coating layers

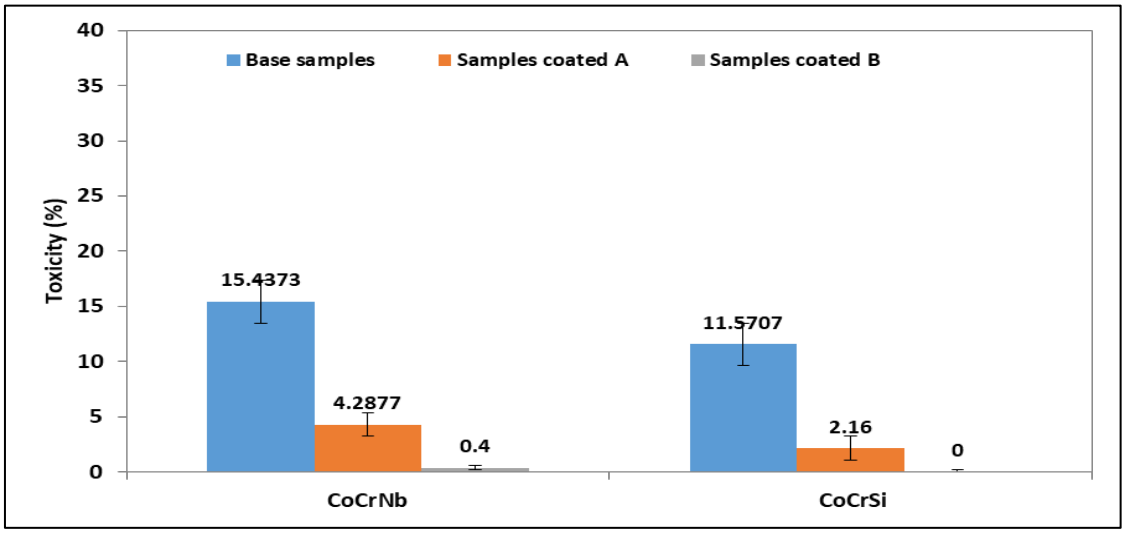

Figure 15: Toxicity of the base (CoCr) and coated samples by two torch flame spray with HAP+SiC (A) and Zeolite+ZrO_2 (B) coating layers

4. Conclusion

CoCr-based alloys with amount of Nb and Si (5wt. %) were developed via powder metallurgy to better understand their behavior for potential applications as biomedical implants. Two torch flame spray process was applied for two types coating (75%HAP+25%SiC) and (75%Zeolite+25%ZrO_2). The Surface characteristics, mechanical properties, corrosion resistance, ions release, Atomic force microscopy were studied of uncoated and coated samples.

The morphology of the CoCr alloy coated with HAP + SiC (type A) is of an irregular kind, and the CoCrNb and CoCrSi coated with Zeolite+ ZrO_2 (type B) are circular type. The use of multiple flame spraying results in a significant level of waviness/roughness in the (HAP+SiC) and (Zeolite+ZrO_2) coating. Due to the enormous stress concentrations at peaks, significant roughness causes corrosion pitting to form. Since the top layer particles that are not distorted in various sizes, samples have varying degrees of roughness. However, the textures of two type coatings are similar in general.

The Zeolite+ZrO_2 and HAP+SiC coating (type A) act as barrier to prevent the release of Co and Cr ions for CoCr-based alloys. CoCrSi coated with (Zeolite+ZrO_2) demonstrates reduced corrosion rate values due to creating a persistent protective layer. Two type coating increased the wear resistance of CoCr based alloy, the orthopaedic applications employ CoCr alloy (CoCrNb, CoCrSi) coated with HAP+SiC when superior wear resistance is required. Using torch flame spray has higher adhesion strength of coating with substrate than single torch flame spray process as in tensile pull-out test.

There is no harmful effect, and cell survival is equal or above 85% of CoCrNb and CoCrSi samples. In general, implants made of CoCrSi coated with (Zeolite+ZrO_2) have a good biocompatibility and cytotoxicity of 0% when placed within the human body.

Author contributions

Conceptualization, N. Abdulkader; and Sh. Jabbar; methodology, N. Abdulkader; and Sh. Jabbar; data analysis, Sh. Jabbar; N. Abdulkader; and P. Ahmed; investigation, N. Abdulkader; and Sh. Jabbar; writing—original draft preparation, Sh. Jabbar; and P. Ahmed; writing—review & editing, Sh. Jabbar; and P. Ahmed; visualization, N. Abdulkader; and Sh. Jabbar; All authors have read and agreed to the published version of the manuscript.

Funding

This research received no specific grant from any funding agency in the public, commercial, or not-for-profit sectors.

Data availability statement

Not applicable.

Conflicts of interest

The authors of the current work do not have a conflict of interest.

References

[1] M. B. Nasab, M. R. Hassan, B. Sahari, Metallic biomaterials of knee and hip: A review, Trends Biomater .Artif. Organs, 24 (2010) 69–82.

[2] Maier, P.; Hort, N. Magnesium Alloys for Biomedical Applications; Multidisciplinary Digital Publishing Institute :Basel, Switzerland, 2020 .

[3] Zhang, S. Hydroxyapatite Coatings for Biomedical Applications; CRC Press: Boca Raton, FL, USA, 2013.

[4] B. Priyadarshini, M. Rama Chetan, U. Vijayalakshmi, Bioactive coating as a surface modification technique for biocompatible metallic implants: A review. J. Asian Ceram. Soc., 7 (2019) 397–406. https://doi.org/10.1080/21870764.2019.1669861

[5] J. Jiang, G. Han, X. Zheng, G. Chen & P. Zhu, Characterization and biocompatibility study of hydroxyapatite coating on the surface of titanium alloy. Surf. Coat. Technol., 375 (2019) 645–651. https://doi.org/10.1016/j.surfcoat.2019.07.067

[6] D. Arcos, and M. V. Regí, Sol–gel silica-based biomaterials and bone tissue regeneration, Acta Biomater, 6 (2010) 2874–2888. https://doi.org/10.1016/j.actbio.2010.02.012

[7] M. Gasik, Understanding biomaterial-tissue inter -face quality: combined in vitro evaluation, Sci. Technol. Adv. Mater., 18 (2017) 550–562. https://doi.org/10.1080/14686996.2017.1348872

[8] Y. Ding, S. Tang, B. Yu, Y. Yan, H. Li, J. Wei, and J. Su, In vitro degradability, bioactivity and primary cell responses to bone cements containing mesoporous magnesium–calcium silicate and calcium sulfate for bone regeneration, J. R. Soc. Interface, 12 (2015)1-10. https://doi.org/10.1098/rsif.2015.0779

[9] X. Wang, H. C. Schröder, M. Wiens, H. Ushijima and W. E. G. Müller, Biosilica and bio-polyphos -phate: applications in biomedicine (bone for -mation), Curr. Opin. Biotechnol., 23 (2012) 570–578. https://doi.org/10.1016/j.copbio.2012.01.018

[10] H.C. Vasconcelos and M.C. Baretto, Tailoring the Microstructure of Sol–Gel Derived Hydroxyapatite/Zirconia Nanocrystalline Composites, Nanoscale Res. Lett., 6 (2011) 2 . https://doi.org/10.1007/s11671-010-9766-z

[11] K. Yoshida, K. Hashimato, Y. Toda, S. Udagawa and T. Kanazawa, J. Eur. Ceram. Soc., 26 (2006) 515-518.

[12] Buzimov, A. Y., et al. Effect of mechanical treatment on properties of zeolites with chabazite structure, J. Phys. Conf. Ser., 790 012004 . 2017. http://iopscience.iop.org/1742-6596/790/1/012004

[13] A. Yasumori , S. Yanagida and J. Sawada , Preparation of a titania/X -zeolite/porous glass composite photocatalyst using hydrothermal and drop coating processes, Molecules, 20 (2015) 2349-2363. https://doi.org/10.3390/molecules20022349

[14] G. A. Naji , R. A. Omar , R. Yahya , A. Dabbagh, Sodalite zeolite as an alternative all-ceramic infiltrating material for alumina and zirconia toughened alumina frameworks, Ceram. Int., 42 (2016) 12253-12261. https://doi.org/10.1016/j.ceramint.2016.04.171

[15] N. Iqbal et al. Nano-hydroxyapatite reinforced zeolite ZSM composites: A comprehensive study on the structural and in vitro biological properties, Ceram. Int., 42 (2016) 7175-7182. https://doi.org/10.1016/j.ceramint.2016.01.107

[16] J.E. Tercero et al., Effect of carbon nanotube and aluminum oxide addition on plasma-sprayed hydroxyapatite coating's mechanical properties and biocompatibility, J. Mater. Sci. Eng., 29 (2009) 2195–2202. http://dx.doi.org/10.1016/j.msec.2009.05.001

[17] L. Zhang, L. Pei, H. Li, S. Li, S. Liu, Y. Guo, Preparation and characterization of Na and F co-doped hydroxyapatite coating reinforced by carbon nanotubes and SiC nanoparticles, Mater. Lett., 218 (2018) 161–164. https://doi.org/10.1016/j.matlet.2018.01.158

[18] M. R. Hosseini, M. Ahangari, M. H. Johar, and S. R. Allahkaram, Optimization of nano HA-SiC coating on AISI 316L medical grade stainless steel via electrophoretic deposition, Mater. Lett., 285 (2021) 129097. http://dx.doi.org/10.1016/j.matlet.2020.129097

[19] S. Mandal, Ceramics for biomedical applications, Biomed. Eng. Appl. Healthc., (2019) 229–247. http://dx.doi.org/10.1007/978-981-13-3705-5_10

[20] A. Abdullah and A. Mohammed, Scanning Electron Microscopy (SEM): A Review Int. Conf. Hydraul. Pneum. - HERVEX, 77–85, 2018.

[21] Standard Test Method for Electrochemical Reactivation (EPR) for Detecting Sensitization of AISI Type 304 and 304L Stainless Steels, ASTM G108-94 (2015).

[22] N.M. Dawood, Erosion-Corrosion Behavior of Al-20%Ni-Al2O3 Metal Matrix Composites by Stir Casting, Mater. Sci. Forum., 1002 (2020) 161-174. http://dx.doi.org/10.4028/www.scientific.net/MSF.1002.161

[23] R. Zdero, L. E. Guenther, and T. C. Gascoyne, Pin-on-Disk Wear Testing of Biomaterials used for Total Joint Replacements, Experimental Methods in Orthopaedic Biomechanics, (2017) 299–311. http://dx.doi.org/10.1016/B978-0-12-803802-4.00019-6

[24] Debdatta R., Recent Advances and Applications of Thermoset Resins 2nd Edition, February 11, 2022.

[25] A. El Hassanin, G. Quaremba, P. Sammartino, D. Adamo, A. Miniello, and G. Marenzi, Effect of implant surface roughness and macro- and micro-structural composition on wear and metal particles released, Materials, (Basel)., 14 (2021) 6800. http://dx.doi.org/10.3390/ma14226800.

[26] I. Dimić , I. Cvijović-Alagić , M. Rakin , B. Bugarski , Analysis of Metal Ion Release From Biomedical, Metall. Mater. Eng., 19 (2013) 167-176 .

[27] E. Al-Hassani, F. Al-Hassani, and M. Najim, Effect of polymer coating on the osseointegration of CP-Ti dental implant, AIP Conf. Proc., 1968 , 030022 (2018). https://doi.org/10.1063/1.5039209

[28] Berzins D. and Brantley W., Adverse effects from orthodontic alloys. Elsevier Ltd, 2017.

[29] C. Domínguez-Trujillo et al., Bioactive coatings on porous titanium for biomedical applications, Surf. Coat. Technol., 349 (2018) 584–592. http://dx.doi.org/10.1016/j.surfcoat.2018.06.037

[30] M. Akhtari-Zavareh et al., Fundamentals and Applications of Thermal Spray Coating, Can. J. Basic Appl. Sci., 5 (2017) 1-11.

[31] Choi A. H., Ben-Nissan B., Bendavid A., and Latella B., Mechanical behavior and properties of thin films for biomedical applications. Elsevier Ltd, 2016.

[32] W. Siswomihardjo, M. K. Herliansyah, and N. Dinar, Biocompatibility of Metal Alloys as Medical Devices, 2017 5th Int. Conf. Instrument.Commun, Inf. Technol. Biomed. Eng., (ICICI-BME), 2017, 10-12. http://dx.doi.org/10.1109/ICICI-BME.2017.8537714